

# Urban Heat Island Study Based on LANDSAT Remote Sensing Images: A Case Study of Tokyo



Rui Wang<sup>1</sup>, Wangchongyu Peng<sup>2</sup>, Wei Chen<sup>2</sup>, Weijun Gao<sup>3</sup>, Soichiro Kuroki<sup>4</sup>

<sup>1</sup> Master Student, Department of Architecture, University of Kitakyushu

<sup>2</sup> PhD Student, Department of Architecture, University of Kitakyushu

<sup>3</sup> Professor, Department of Architecture, University of Kitakyushu

<sup>4</sup> Emeritus Professor, Department of Architecture, University of Kitakyushu

人口過密と産業の集積、そこへ地球温暖化の影響も加わって急速に進む大都市のヒート・アイランド現象。そのメカニズムを、アジアを代表する大都市・東京を例に、LANDSATの観測画像をもとに解明する。

## Abstract

The urban is the center of regional society, economy, politics and culture. And the urban is a symbol of human civilization and development. Urbanization is a common trend in many countries. In developing countries, this situation is particularly evident. With rapid urbanization, there are lots of environment problems. Among these environmental problems, the urban heat island effect is the most important. Urban heat island has deep impacts on material cycles and energy transfers within urban ecosystems and has become an important issue in urban climate and environmental research. This paper, based on the Multi-time-phase TM /ETM+ Remote Sensing images, takes Tokyo as an example to contrast four-time inversions results and study the evolution rule and the characteristic of the heat island effect with Single-Channel Algorithm. Through this study, we can find the evolution law of urban heat island in Tokyo. And then for the future development of cities and solutions to the urban heat island effects, it can provide a more effective way of train of thought and methods.

## Keywords

Urban Heat Island, ArcGIS; Remote Sensing; Urban Heat Island; Land Surface Temperature

## Introduction

With the rapid urbanization, there has been a tremendous growth in population and buildings in the urban. The urbanization has a great impact on the environment in the urban, especially, the thermal environment. It is shown on the rising air-temperature in the center of the urban. And the suburbs air-temperature is at least two degrees lower than the urban. On the spatial distribution of temperature, the urban is like an island. So, we call it the urban heat islands (UHI). (Shown in Fig.1)

The cause of the UHI is wide-ranging. For one thing, it's caused by nature. Such as some special landform condition and climatic condition. For another, the most important is the development of human society. Entering the 21th century, because of urban extension, population concentration, developed industry,

traffic jams and air pollution, and most of the buildings in the urban are made of concrete with low heat capacity and high heat

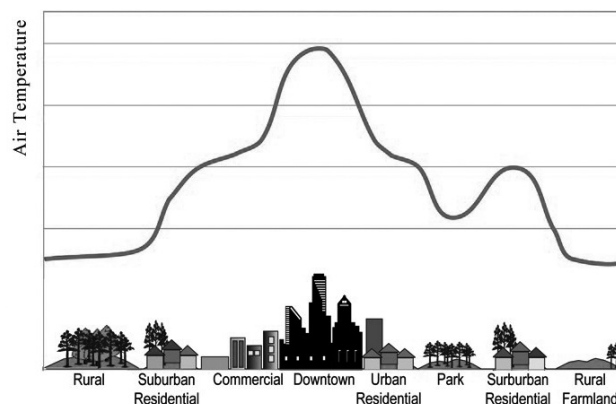


Fig. 1. Diagram of Urban Heat Island

conductivity, at the same time, high-rise building will weaken the wind, the temperature in the urban will be higher. Conversely, in sub-urbans, there aren't so many buildings and population. So, the environment is closer to nature and in stark contrast to that in the urban. It leads to the UHI effect highlighting.

The urban heat island is an important problem for the urban planning because there are many indications that UHIs have several negative impacts on an urban environment. With the air-temperature increasing, air will rise, and there will be a low-pressure vortex at central area of the urban. Then the pollutants, such as sulfur oxides, nitrogen oxides, carbon oxides, hydrocarbons, etc. produced by daily life, vehicles and factory will be gathered in the urban and damage people's health. Next, because of the pollutant, the temperature will rise further. Finally, it will be a vicious cycle, and generate even more serious social problems.

## Research Region

Tokyo, officially Tokyo Metropolis, is the capital city of Japan. The mainland portion of Tokyo lies northwest of Tokyo Bay and measures about 90 km east to west and 25 km north to south. Chiba Prefecture borders it to the east, Yamanashi to the west, Kanagawa to the south, and Saitama to the north. Tokyo has an area of about 2188 square kilometers with a population of about 37 million, including urban area of about 621 square kilometers with a population of 13.74 million. The Tokyo Metropolitan Government administers the 23 Special Wards of Tokyo. In addition, Tokyo also includes 26 more cities, 5 towns, and 8 villages, each of which has a local government. (Shown in Fig.2)

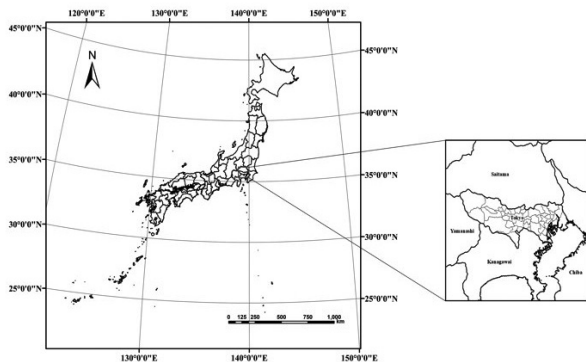


Fig. 2. Research Region

The Greater Tokyo Area is the most populous metropolitan area around the world. And at the same time, Tokyo has the largest metropolitan economy in the world. According to a study conducted, the Tokyo urban area had a total GDP of \$2 trillion in 2012, that topped in the list. Tokyo is also a major international finance center. About the transportation, Tokyo is Japan's largest domestic and international hub for rail, ground, and air transportation.

Tokyo is a temperate monsoon climate with an annual average air-temperature of 15.6 degrees. It has 4 distinctive seasons with abundant precipitation. There is more precipitation in summer because of the southeastern monsoon. There is less snow in winter.

Considering the characteristics of remote sensing image processing software and corresponding data collection, in this research, we selected The Imperial Palace as the center, and chose a circle area with a radius of 50 kilometers in Tokyo. The total area of research region is about 7853.98 square kilometers, including the most parts of the Tokyo Metropolitan Area. And it can typically reflect the evolution of the urban heat island in Tokyo. The satellite image is shown in Fig.3.



Fig. 3. The Satellite Image of Research Region

## Research Data

The remote sensing data used in this research is Landsat 4-5

TM (Thematic Mapper) and Landsat 8 OLI (Operational Land Imager)/TIRS (Thermal Infrared Sensor) of Tokyo in March from 1985 to 2015 (shown in Table 1). And the orbital number is 107/35.

Table 1. Images used in this research

Sensor	Data
Landsat-5	1985-03-28
Landsat-5	1995-03-08
Landsat-5	2005-03-19
Landsat-8	2015-03-31

The Landsat Thematic Mapper (TM) sensor was carried onboard Landsat 4 and 5 from July 1982 to May 2012 with a 16-day repeat cycle. And the Landsat 5 TM image data files consist of 7 spectral bands. The resolution is 30 meters for Band 1 to 7. Among them, Band 6, the Thermal infrared, was collected at 120 meters, but was resampled to 30 meters. The approximate scene size is 170 kilometers north-south by 183 kilometers east-west.

The Operational Land Imager (OLI) and Thermal Infrared Sensor (TIRS) are instruments onboard the Landsat 8 satellite, which was launched in February of 2013. The satellite collects images of the Earth with a 16-day repeat cycle. And the Landsat 8 OLI/TIRS image data files consist of nine spectral bands with a spatial resolution of 30 meters for Bands 1 to 7 and 9. The ultra-blue Band 1 is useful for coastal and aerosol studies. Band 9 is useful for cirrus cloud detection. The resolution for Band 8 (panchromatic) is 15 meters. Thermal bands 10 and 11 are useful in providing more accurate surface temperatures and are collected at 100 meters. The approximate scene size is 170 km north-south by 183 km east-west.

The weather of data that we selected was sunny. The visibility in the study area is high. And the imaging quality chosen is good. And the software used for the study is ArcGIS 10.3.

## Research Method

Land surface temperature is an important parameter for many research applications. And I used Single- Channel Algorithm for automatic retrieval of brightness temperature, land surface emissivity and land surface temperature from Landsat data to estimate land surface temperature.

This method can be used in order to process both Landsat-5

TM and Landsat-8 OLI/TRIS data. It consists of 3 separate steps, namely, NDVI Thresholds, Thermal Band to Brightness Temperature and Retrieve LST (Land Surface Temperature).

### 1. NDVI Thresholds

This step estimates land surface emissivity employing Normalized Difference Vegetation Index Thresholds Method (NDVI<sup>THM</sup>) to distinguish between soil pixels (NDVI < NDVI<sub>S</sub>), full vegetation pixels (NDVI > NDVI<sub>V</sub>) and mixed pixels (NDVI<sub>S</sub> ≤ NDVI ≤ NDVI<sub>V</sub>). And the threshold values of NDVI<sub>S</sub> = 0.2 and NDVI<sub>V</sub> = 0.5 make the method applicable for global conditions. The NDVI can be calculated from Landsat 4, 5 and 7 by equation 1 and Landsat 8 by equation 2. And then Normalized Difference Vegetation Index (NDVI) are converted to Land Surface Emissivity (LSE) using modified NDVI<sup>THM</sup>.

$$NDVI = \frac{Band4 - Band3}{Band4 + Band3} \quad (1)$$

$$NDVI = \frac{Band4 - Band5}{Band4 + Band5} \quad (2)$$

In the conversion, the emissivity ( $\epsilon$ ) of soil and full vegetation pixels should be used. And the emissivity can be defined by user. In general, the default emissivity values are:

*soil pixels:*

$$\epsilon = \epsilon_{S\lambda} = 0.96$$

*full vegetation pixels:*

$$\epsilon = \epsilon_{V\lambda} + C_{\lambda} = 0.985 + 0.05 = 0.99$$

The emissivity of mixed pixels is calculated by equation 3. Each pixel ( $P_V$ ) is calculated by equation 4 considering the proportion of vegetation. And the cavity effect ( $C_{\lambda}$ ) that due to surface roughness is calculated by equation 5. In this equation, the geometrical factor ( $F'$ ) is the mean value 0.55.

$$E = E_{V\lambda} \cdot P_V + E_{S\lambda} \cdot (1 - P_V) + C_{\lambda} \quad (3)$$

$$P_V = \left( \frac{NDVI - NDVI_S}{NDVI_V - NDVI_S} \right)^2 \quad (4)$$

$$C_{\lambda} = (1 - E_{S\lambda}) \cdot \epsilon_{V\lambda} \cdot F' \cdot (1 - P_V) \quad (5)$$

Additionally, this step allows the user to define the emissivity for the surface water. Normally, the default emissivity is 0.99. Before then, water bodies mask and the subset area (polygon feature layer) must be defined.

## 2. Thermal Band DN to Brightness Temperature

The next step is using appropriate conversion coefficients (gain and bias) to convert pixel values of Landsat thermal band (Band 6) to at-sensor spectral radiance in  $W \cdot m^{-2} \cdot sr^{-1} \cdot \mu m^{-1}$  according to equation 6 and then transforming  $L_s$  to at-sensor brightness temperature ( $T_s$ ) applying inverted Planck's Law and specific calibration constants ( $K_1$  and  $K_2$ ) as in the equation 7. And this step can only work with LPGS (Level-1 Product Generation System) data.

$$L_s = gain \cdot DN + bias \quad (6)$$

$$T_s = \frac{K_2}{\ln\left(\frac{K_1}{L_s} + 1\right)} \quad (7)$$

## 3. Retrieve LST

This step estimates LST (Land Surface Temperature) with S-C (Single-Channel) Algorithm according to equation 8a, 8b and 8c.

$$LST = \gamma \left[ \frac{1}{\epsilon} (\psi_1 L_s + \psi_2) + \psi_3 \right] + \delta \quad (8a)$$

$$\gamma = \left[ \frac{c_2 L_s}{T_s^2} \left( \frac{\lambda^4 L_s}{c_1} + \frac{1}{\lambda} \right) \right]^{-1} \quad (8b)$$

$$\delta = -\gamma \cdot L_s + T_s \quad (8c)$$

In these equations, the necessary data are: the calculated brightness temperature ( $T_s$ ) and the land surface emissivity ( $\epsilon$ ) datasets as well as some specific atmospheric functions ( $AF$ ). The AF's ( $\psi_1$ ,  $\psi_2$  and  $\psi_3$ ) are used for correction of the atmosphere influence which is very important part of the LST retrieval algorithm. The AF's are computed from atmospheric parameter with equation 9a, 9b and 9c.

$$\psi_1 = \frac{1}{\tau} \quad (9a)$$

$$\psi_2 = -L^\downarrow - \frac{L^\uparrow}{\tau} \quad (9b)$$

$$\psi_3 = L^\downarrow \quad (9c)$$

In these equations,  $\tau$  is atmospheric transmissivity,  $L^\uparrow$  is up-welling atmospheric radiance, and  $L^\downarrow$  is down-welling atmospheric radiance. The site-specific atmospheric parameters can be calculated by means of an atmospheric radiative transfer model, such as ACPC (Atmospheric Correction Parameter Calculator that is a freely accessible web based on MODTRAN interface). The S-C Algorithm uses also Planck's radiation constants ( $c_1 = 1.19104 \cdot 10^8 W \cdot \mu m^4 \cdot m^{-2} \cdot sr^{-1}$ ;  $c_2 = 1.43877 \cdot 10^4 \mu m \cdot K$ ) and the effective wavelength of Landsat-5 TM and Landsat-8 OLI/TRIS Band 6.

These three steps are the whole procedure of land surface temperature retrieval from Landsat data.

Using this method, we can invert the land surface temperature. And then, through ArcGIS, the air temperature pattern of Tokyo can be gotten. The urban heat island effect is obvious in air temperature pattern. And we can find the evolution rule of urban heat island effect in Tokyo in the past several years.

## Result and Analysis

According to the above research method, Landsat-5 TM images and Landsat-8 OLI/TRIS images are converted into the distribution maps of Tokyo land surface temperature in March 28th 1985, March 8th 1995, March 19th 2005 and March 31st 2015 (following show with 1985,1995, 2005 and 2015) In the distribution maps, the red area is the high-temperature zone, namely urban heat island area, and the blue area is the low-temperature zone. The more different in color between two regions, the more different in temperature between these regions.

### 1. Land Surface Temperature and Urban Heat Island Analysis in 1985

Fig.4 shows the distribution of land surface temperature on March 28th 1985.

Fig.5 shows the frequency distribution curve of land surface temperature on March 28th 1985.

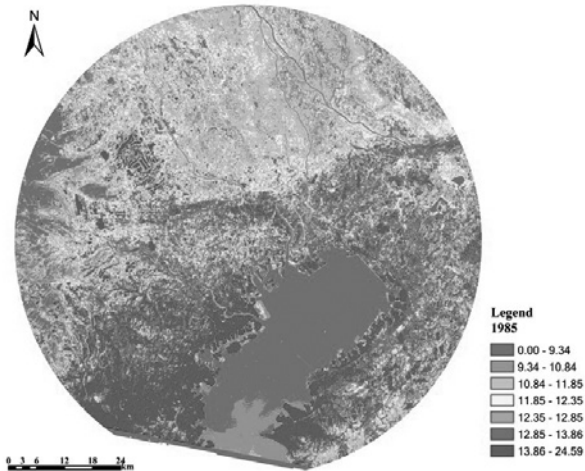


Fig. 4. The Distribution of LST (1985-03-28)

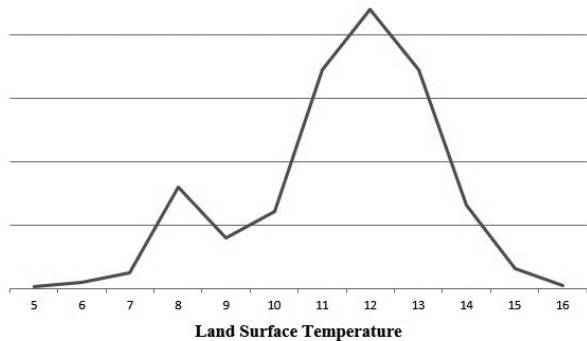


Fig. 5. The Frequency distribution curve of Land Surface Temperature (1985-03-28)

According to the above two figures, the mean of land surface temperature in 1985 is about 11.44 degrees. The urban heat island is not obvious in the center of Tokyo. And the land surface temperature in the region between Tokyo and Yokohama is commonly higher than that in the other region. And the region with high temperature. The land surface temperature around the Tokyo Bay is higher than that of inland area. Through Fig.5, we can find the temperature is centered on the range of 10 degrees to 11 degrees. And the maximum temperature difference is about 4 degrees.

## 2. Land Surface Temperature and Urban Heat Island Analysis in 1995

Fig.6 shows the distribution of land surface temperature on March 8th 1995.

Fig.7 shows the frequency distribution curve of land surface temperature on March 8th 1995.

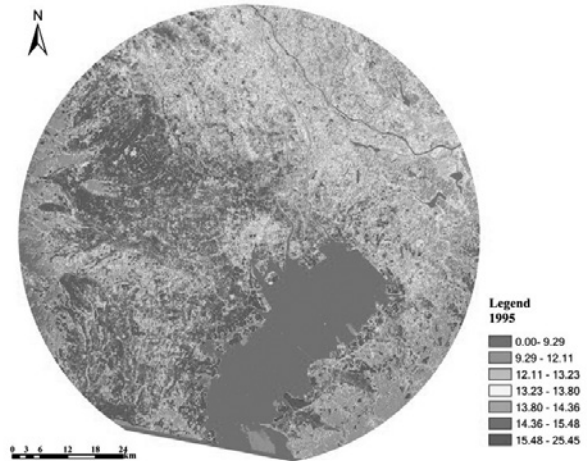


Fig. 6. The Distribution of LST (1995-03-08)

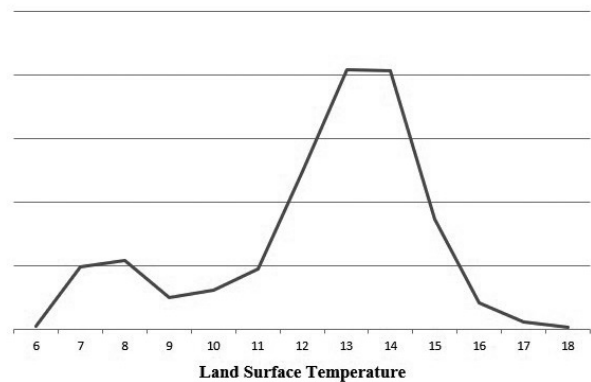


Fig. 7. The Frequency distribution curve of Land Surface Temperature (1995-03-08)

According to the above two figures, the mean of land surface temperature in 1995 is about 12.39 degrees. The urban heat island is formed in the northwest of the center of Tokyo. But, because of vegetation in The Imperial Palace, comparing to the neighboring regions, the land surface temperature is lower. And at the same time, the region that the land surface temperature was very high in 1985, between Tokyo and Yokohama, is cooling. And the north area is still very cool in 1995. Through Fig.7, the frequency distribution curve of land surface temperature in 1995 is similar to that in 1985. But the temperature is centered on the range of 13 degrees to 14 degrees. And the maximum

temperature difference is over 4 degrees. It means that the urban heat island is becoming more serious.

### 3. Land Surface Temperature and Urban Heat Island Analysis in 2005

Fig.8 shows the distribution of land surface temperature on March 19th 2005.

Fig.9 shows the frequency distribution curve of land surface temperature on March 19th 2005.

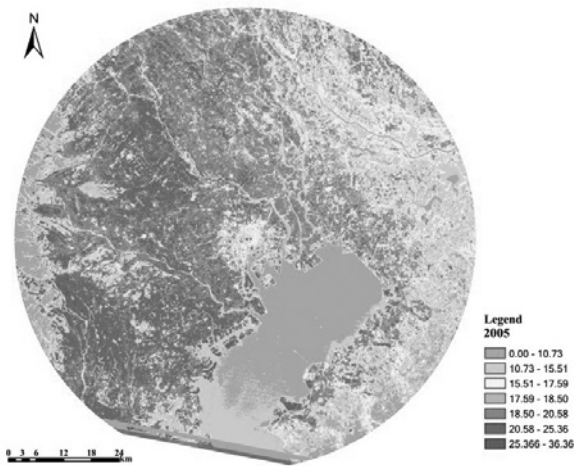


Fig. 8. The Distribution of LST (2005-03-19)

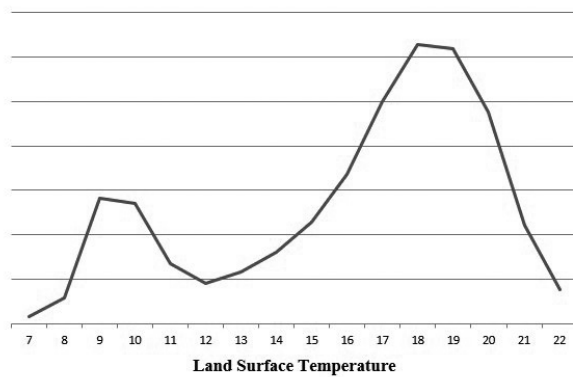


Fig. 9. The Frequency distribution curve of Land Surface Temperature (2005-03-19)

According to the above two figures, the mean of land surface temperature in 2005 is about 16.27 degrees. Comparing to the distribution of land surface temperature in 1995, the area of the region who's the land surface temperature is very high expands obviously, including the north region, the west region and the

northwest region. And in these 10 years, the region between Tokyo and Yokohama is warm again. In a word, the whole west region of the Tokyo center is at a high-temperature area. And the east region can still keep cool. And the center of Tokyo always keeps at a relatively low-temperature level. With ten years construction, the land surface temperature of all region is higher. And the temperature is centered on the range of 17 degrees to 19 degrees. And we can also find that the maximum temperature difference is bigger, to about 6 degrees.

### 4. Land Surface Temperature and Urban Heat Island Analysis in 2015

Fig.10 shows the distribution of land surface temperature on March 31st 2015.

Fig.11 shows the frequency distribution curve of land surface temperature on March 31st 2015.

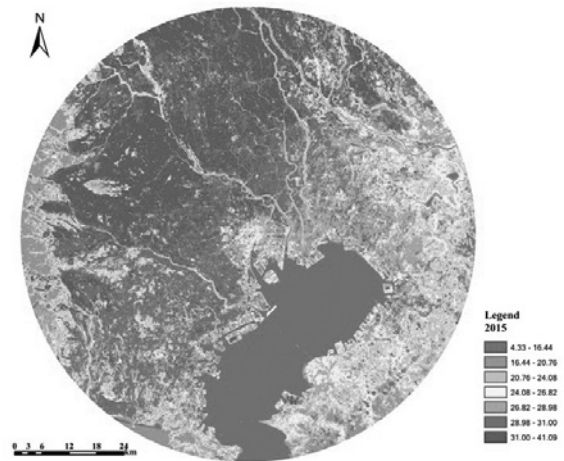


Fig. 10. The Distribution of LST (2015-03-31)

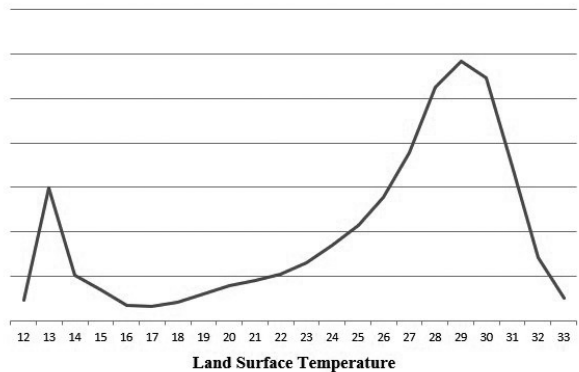


Fig. 11. The Frequency distribution curve of Land Surface Temperature (2015-03-31)

According to the above two figures, the mean of land surface temperature in 2015 is about 25.55 degrees. It's obvious that the mean of land surface temperature is much higher than before. The north region and northwest region of Tokyo center are becoming the central area of the urban heat island. In these regions, high-temperature areas are very intensive, and at the same time, there is a trend towards the east region of Tokyo center. Due to the influence of the marine environment and mainly the vegetation of the Imperial Palace, the center of Tokyo, the Imperial Palace and the surrounding area is still at a low-temperature area. But the mean of land surface temperature rises a lot comparing to 10 years ago. Although the mean temperature of the whole research area has increased a lot, the maximum temperature difference doesn't change too much. It means that the urban heat island is not deteriorated by the rise of land surface temperature in the past ten years.

## Conclusion

- 1) In the thirty years, the urban heat island in Tokyo and the surrounding area is more serious and obvious, especially at the first 20 years. In last 10 years, the urban heat island is relatively controlled effectively.
- 2) The mean of land surface temperature rose faster and faster, especially after twenty-first century in March.
- 3) Because of the rapid development of cities and the rapid expansion of population, the area of urban heat island is also expanding. But, at the same time, due to the influence of natural environment, the development speed of urban heat island to east region and west region is slow. And the development speed to north is very fast.
- 4) The Imperial Palace and surrounding area always stay at a low-temperature area, because of the vegetation in the Imperial Palace and the marine environment.
- 5) By comparison, it is not difficult to find that the relationship between urban heat island and population activities. The more frequent the population activities are, the more serious the urban heat island effect is. Conversely, the less the population is, the less obvious the urban heat island is.
- 6) Comparison of actual land use, vegetation can effectively reduce land surface temperature and mitigate the urban heat island.

## References

- 1) Liang Y T, Chen Z H, Xia Z H. Decades Change and Mechanism of the Urban Heat Island Effect in Wuhan Based on RS and GIS. *Resources and Environment in the Yangtze Basin*. 2010,08: 14-918
- 2) Fujio K, Shunji T. The Effects of Land-use and anthropogenic Heating on the Surface Temperature in the Tokyo Metropolitan Area: A Numerical Experiment. *Atmospheric Environment*. 1991,25:155-164
- 3) Yng Y B, Su W Z, Jiang N. Application of Remote Sensing to Study Urban Heat Island Effect. *Geography and Geo-Information Science*. 2016,05:36-40
- 4) S Bonafoni, G Baldinelli, P Verducci. Sustainable strategies for smart cities: Analysis of the town development effect on surface urban heat island through remote sensing methodologies. *Sustainable Cities and Society*. 2017,29:211-218
- 5) J P Walawender, M J Hajto, P Iwaniuk. A new ArcGIS toolset for automated mapping of Land Surface Temperature with the use of LANDSAT satellite data. *IEEE IGARSS*. 2012:4371-4374
- 6) Hideki Takebayashi, Masashi Senoo. Analysis of the relationship between urban size and heat island intensity using WRF model. *Urban Climate*. 2017
- 7) Y. Hirano, T. Fujita. Evaluation of the impact of the urban heat island on residential and commercial energy consumption in Tokyo. *Energy*. 2012,37:371-383
- 8) LI Z Q, GONG C L, HU Y, YIN Q, KUANG D B. The Progress of the Remote Sensing Research on Urban Heat Island. *Remote Sensing Information*. 2009,04:100-105
- 9) D A QUATTROCHI, J C LUVALL. Application of high-resolution thermal infrared remote sensing and GIS to assess the urban heat island effect. *Remote Sensing*. 1997,18:287-304
- 10) HU H L, CHEN Y H, GONG A D. A Quantitative Study of the Relationship between Urban Vegetation and Urban Heat Island. *Remote Sensing for Land & Resources*. 2005,03:5-13